Phase behavior of charged lipid bilayer membranes with added electrolyte

Shigeyuki Komura,[a] Hisashi Shirotori, and Tadashi Kato
Department of Chemistry, Faculty of Science, Tokyo Metropolitan University, Tokyo 192-0397, Japan

(Received 3 February 2003; accepted 11 April 2003)

We investigate the phase behavior of the aqueous solution of charged lipid bilayer membranes forming a lamellar structure in the presence of the added electrolyte. The Goldstein–Leibler model [Phys. Rev. A **40**, 1025 (1989)] proposed for neutral lipids is extended by taking into account the screened electrostatic interaction which belongs to the so called intermediate region of the Poisson–Boltzmann theory. We mainly focus on the variation of the phase behavior as the added electrolyte concentration is changed. By decreasing the electrolyte concentration, the electrostatic repulsion between the neighboring membranes becomes stronger. As a result, the maximum equilibrium swelling composition shifts to larger water content, and the lamellar repeat distance increases although the membrane thickness remains almost constant. Our results recover not only the experimentally observed phase diagram for the charged lipid, but also the dependence of the lamellar repeat distance both on the electrolyte concentration and on the lipid composition. Some discussions are provided for the case when the electrostatic interaction is not screened due to the absence of any electrolyte. © *2003 American Institute of Physics.* [DOI: 10.1063/1.1579675]

I. INTRODUCTION

Lipids are amphiphilic molecules with a hydrophilic head group and usually two lipophilic hydrocarbon chains. Phase diagrams for a binary system consisting of lipid and water have been studied with a variety of experimental techniques.[1] One of the typical structures observed in such a binary system is a lamellar structure which is formed due to the amphiphilic nature of the lipid molecule.[2] The structure of hydrated lipid bilayer membranes are good model systems for the study of interacting membranes. The lamellar phase is fluid at high temperature (the so-called L_α phase), whereas at low temperature, the bilayers become a two-dimensional gel ($L_{\beta'}$ phase). On the other hand, both the L_α and $L_{\beta'}$ phases can take up only a restricted amount of water. Adding more water leads to a phase separation between the lamellar phase and excess water. As for the electrostatically neutral lipids, these phase behaviors can typically be observed in the dimyristoyl phosphatidylcholine (DMPC)/water binary system.[3] Recently it was reported that the sorption of water triggers a first-order transition from the $L_{\beta'}$ to the L_α phase.[4]

In contrast to the neutral lipids, such as phosphatidylcholine (PC) or phosphatidylethanolamines (PE), much less is known about the phase behavior of charged lipid bilayer membranes although several attempts have been made. For example, force measurement between egg lecitin bilayers containing various amounts of the charged phosphatidylglycerol (PG) and phosphatidylinositol (PI) was performed using an osmotic stress technique and x-ray diffraction.[5] In this experiment, it was claimed that hydration repulsion dominates out to about 20 to 30 Å separation, whereas more slowly decaying electrostatic repulsion dominates beyond about 30 Å. Concerning the added electrolyte, effects of monovalent ion binding and screening on electrostatic forces have been also investigated by employing the osmotic stress technique.[6] In this work, the binding affinity series onto the charged lipid bilayers of phosphatidylglycerol (PG) and phosphatidylserine (PS) were determined for various cations.

The temperature-composition phase diagram of an anionic dimyristoyl phosphatidylserine (DMPS)/water binary system in the presence of ammonium phosphate has been studied by Hauser *et al.* using x-ray diffraction and differential scanning calorimetry.[7,8] In this system, the L_α to $L_{\beta'}$ transition (the so-called ''main transition'') occurs at progressively lower temperatures as the water content is increased. The lamellar bilayer repeat distance becomes continuously larger with increased water content up to more than 50 wt %. Although the multilayer stacking may be disordered above this water composition, the system does not phase separate up to very high water contents.[9] When the system is diluted more than 70 wt %, there is a transition from a single swollen lamellar phase to a two-phase system consisting of unilamellar vesicles and excess water. Notice that the corresponding equilibrium swelling composition for neutral PC is at most 40 wt %.[3] This difference in the swelling limit implies that the electrostatic repulsion acts to stabilize the swollen lamellar phase.

In the subsequent work by Hauser and Shipley, the effect of monovalent cations on the phase behavior of DMPS as well as other homologous series was studied.[10] According to the x-ray diffraction data, they showed that the main transition temperature increases only slightly upon the addition of NaCl up to 1 M concentration. This means that no major change in lipid packing within a bilayer occurs for this electrolyte concentration regime. The more significant effect of added electrolyte is the pronounced decrease in the lamellar periodicity due to the salt-induced exclusion of aqueous buffer from the intermembrane region. In Ref. 11, it was shown that the addition of higher NaCl concentration up to 6 M increases the main transition temperature significantly.

[a]Electronic mail: komura@comp.metro-u.ac.jp

From the theoretical point of view, the effects of membrane interactions on the structural phase transition of neutral lipid bilayers have been studied by Goldstein and Leibler.[12,13] In their model, the main transition in an isolated bilayer is described by a Landau theory in which the membrane thickness is taken as a coarse-grained order parameter. On the other hand, the dominant molecular intermembrane forces acting between bilayers are considered within a continuum treatment.[14,15] Both of these ''internal'' and ''external'' degrees of freedom of the membranes are coupled to each other when the typical distance between the membranes is comparable to their thickness. For neutral phospholipid lamellae, the long-range van der Waals attraction and short-range hydration repulsion were taken into account. Therefore it is natural to include the electrostatic repulsion in the Goldstein–Leibler theory to investigate the phase behavior of charged membranes.

A detailed discussion of the electrostatic properties of membranes within the Poisson–Boltzmann theory is given in Ref. 16. When an electrolyte is added to the solution, the electrostatic properties (e.g., electric potential, ionic concentration profiles) are strongly screened. The diffusive layers of ions in the solution is characterized by the Debye–Hückel screening length Λ_{D}. In this article, we consider the case when the separation between the membrane is large compared to Λ_{D}, and the coupling between the two membranes is weak. This limit is called as the intermediate region of the Poisson–Boltzmann theory.[16] We will show later that this is really the case in the typical experiments. The main purpose of this article is to calculate the phase diagrams of the aqueous solution of charged lipid bilayer membranes in the presence of the added electrolyte. We pay attention to the variation of the phase behavior as the added electrolyte concentration is changed. By decreasing the electrolyte concentration, we show that the maximum equilibrium swelling composition shifts to larger water content. Then the lamellar repeat distance increases simultaneously although the membrane thickness remains almost the same.

This article is constructed as follows: In the next section, we first review the Goldstein–Leibler theory,[13] and explain the newly added electrostatic interaction in the presence of electrolyte.[16] Based on this generalized model, we then describe how we calculated the phase diagrams. In Sec. III, we present the calculated results which will be compared with those from the previous experimental works. Some discussions are provided in Sec. IV.

II. MODEL

As a starting point of the present study, we first describe the Goldstein–Leibler theory briefly.[13] Consider a mixture of N_ℓ lipids and N_{w} water molecules in volume $\Omega = N_\ell v_\ell + N_{\mathrm{w}} v_{\mathrm{w}}$, where v_ℓ and v_{w} are molecular volumes of lipid and water, respectively. The volume fraction of lipid is then $\phi = N_\ell v_\ell / \Omega$. As shown in Fig. 1, the multilamellar lattice is assumed to be composed of sharply defined aqueous and membrane regions of thickness d and δ, respectively (Luzzati approximation). For such a stack of lamellae, the incompressibility condition is given by

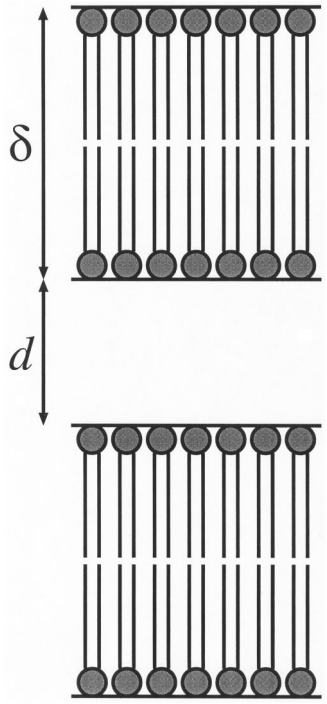

FIG. 1. The geometry of the lamellar stack. The multilamellar lattice is assumed to be composed of sharply defined aqueous and membrane regions of thickness d and δ, respectively.

$$\frac{\delta}{d} = \frac{\phi}{1-\phi}. \tag{1}$$

In order to describe the main transition in an isolated bilayer, we introduce an order parameter defined by

$$\psi \equiv \frac{\delta - \delta_0}{\delta_0}, \tag{2}$$

where δ_0 is the thickness in the L_α phase coexisting with excess water. This order parameter is nonzero in the $L_{\beta'}$ phase, whereas it is small in the L_α phase. Since the structural main transition between the L_α and $L_{\beta'}$ phases is a first-order transition, the Landau expansion of the stretching free energy per lipid molecule is expressed as

$$F_{\mathrm{L}}(\psi, T) = \tfrac{1}{2} a_2(T) \psi^2 + \tfrac{1}{3} a_3 \psi^3 + \tfrac{1}{4} a_4 \psi^4, \tag{3}$$

where T is the temperature, and $a_4 > 0$ for stability. The inequality $a_3 < 0$ is required in order to ensure the thicker $L_{\beta'}$ phase. The temperature dependence of $a_2(T)$ is provided by $a_2(T) \approx a_2'(T - T_0)$, where T_0 is the temperature at which the transition from L_α to $L_{\beta'}$ is critical if the cubic term is absent. With these conditions, the main transition temperature T_{m} is given by

$$T_{\mathrm{m}} = T_0 + \frac{2a_3^2}{9a_2' a_4}. \tag{4}$$

It is believed that the lipid molecules are tilted in the $L_{\beta'}$ phase.[1,2] Since ψ does not describe any intramembrane symmetry differences, however, we do not distinguish between the tilted $L_{\beta'}$ phase and the untilted L_β phase hereafter. In

order to describe such an intramembrane symmetry difference, one needs to include additional order parameters as mentioned in Ref. 13.

For electrostatically neutral bilayers, there are two contributions to the interaction energy per unit area of the membrane.[14,15] The first one is the long-range van der Waals attraction $V_d(\delta,d)$:

$$V_d(\delta,d)=-W\left[\frac{1}{d^2}-\frac{2}{(d+\delta)^2}+\frac{1}{(d+2\delta)^2}\right], \tag{5}$$

where W is the Hamaker constant. The second one is the short-range hydration repulsion $V_h(d)$:

$$V_h(d)=H\exp(-d/\Lambda_h), \tag{6}$$

where H is the amplitude and Λ_h is the decay length. To investigate the phase behavior of the aqueous solution of the neutral bilayer membranes consisting of DMPC, Goldstein and Leibler analyzed the total free energy[13]

$$F_n=N_\ell F_L(\psi,T)+\frac{N_\ell v_\ell}{\delta}[V_d(\delta,d)+V_h(d)]. \tag{7}$$

Notice that $2v_\ell/\delta$ is the area per lipid head group. The internal and the external degrees of freedom of the membranes are coupled through the incompressibility condition (1). Using the above free energy, Goldstein and Leibler were able to calculate the temperature-composition phase diagram which is in semiquantitative agreement with the experimental results for the neutral DMPC/water binary system.[3] An evaluation of relative importance of the various interactions for DMPC bilayers was later discussed in Ref. 17.

Next we consider the interacting charged lipid bilayer membranes in aqueous solution. In the presence of added electrolyte, it is useful to separate the general solution of the appropriate Poisson–Boltzmann equation into several limits in which approximate potential energies can be calculated analytically. In this problem, three important length scales exist: (i) the spacing between the two membranes d; (ii) the Debye–Hückel screening length for 1:1 electrolyte (in SI base unit)

$$\Lambda_D=\left(\frac{\varepsilon_0\varepsilon_w k_B T}{2n_0 q^2}\right)^{1/2}, \tag{8}$$

where ε_0 is the vacuum permittivity, ε_w is the dielectric constant of the aqueous solution, k_B is the Boltzmann constant, n_0 is the number density (per unit volume) of the added electrolyte, and $q>0$ is the electron unit; and finally (iii) the Gouy–Chapman length given by

$$b=\frac{2\varepsilon_0\varepsilon_w k_B T}{q|\sigma|}, \tag{9}$$

where σ is the surface charge distribution assumed to be negative. As argued in Refs. 16, 18, and 19, the dimensionless parameter space $(\Lambda_D/d, b/d)$ can be divided into four asymptotic regions. Among these, we consider the so-called intermediate region in which the relation $b\ll\Lambda_D\ll d$ is satisfied. This is the case where the separation between the membranes d is large compared to the Debye–Hückel screening length Λ_D, whereas the coupling between the two membranes is weak. In such a limit, the electrostatic interaction energy per unit area of the membrane has the following asymptotic form[16]

$$V_e(d)=\frac{32\varepsilon_0\varepsilon_w(k_B T)^2}{q^2\Lambda_D}\exp(-d/\Lambda_D). \tag{10}$$

By assuming complete dissociation, the area per phospholipid head group is about $66\times10^{-20}\,\mathrm{m}^2$ for PS.[6] Then the Gouy–Chapman length (9) is calculated to be $b\approx1.5\times10^{-10}\,\mathrm{m}$ with the use of the other numerical values listed below. For a typical electrolyte concentration, this is relatively small compared to the values of d or Λ_D in the experiment. After the calculation, we will also see that Λ_D is indeed smaller than d, which is reasonably satisfied in the real system. These considerations justify our assumption of the intermediate region.

Using the above asymptotic form of the electrostatic free energy (10), we consider the following total free energy for the charged bilayer membranes

$$F_c=N_\ell F_L(\psi,T)+\frac{N_\ell v_\ell}{\delta}[V_d(\delta,d)+V_h(d)+V_e(d)], \tag{11}$$

which is a straightforward generalization of (7). Here we define the reduced free-energy density $f_c(\phi,T;\psi)\equiv F_c v_\ell/\Omega$ and the reduced parameters by

$$\begin{aligned}&\lambda_h\equiv\frac{\Lambda_h}{\delta_0},\quad \lambda_D\equiv\frac{\Lambda_D}{\delta_0},\\ &w\equiv\frac{W v_\ell}{\delta_0^3},\quad h\equiv\frac{H v_\ell}{\delta_0},\quad e\equiv\frac{32\varepsilon_0\varepsilon_w(k_B T)^2 v_\ell}{q^2\lambda_D\delta_0^2}.\end{aligned} \tag{12}$$

Using the incompressibility condition (1) and the definition of the order parameter (2), we obtain

$$\begin{aligned}f_c(\phi,T;\psi)=\phi&\left[\frac{1}{2}a_2'(T-T_0)\psi^2+\frac{1}{3}a_3\psi^3+\frac{1}{4}a_4\psi^4\right]\\&-\frac{wC(\phi)}{(1+\psi)^3}+\frac{h\phi}{1+\psi}\exp[-D(\phi)(1+\psi)]\\&+\frac{e\phi}{1+\psi}\exp[-E(\phi)(1+\psi)],\end{aligned} \tag{13}$$

where

$$\begin{aligned}&C(\phi)\equiv\frac{2\phi^5(3-\phi^2)}{(1-\phi^2)^2},\quad D(\phi)\equiv\frac{1-\phi}{\lambda_h\phi},\\&E(\phi)\equiv\frac{1-\phi}{\lambda_D\phi}.\end{aligned} \tag{14}$$

The reduced chemical potential is defined by

$$\mu(\phi,T;\psi)=\left[\frac{\partial f_c(\phi,T;\psi)}{\partial\phi}\right]_{T,\psi}. \tag{15}$$

TABLE I. Numerical values of model parameters.

$\delta_0 = 3.5\times10^{-9}$ m	$v_\ell = 1.1\times10^{-27}$ m^3
$a_2' = 2.4\times10^{-21}$ J K^{-1}	$a_3 = -9.3\times10^{-19}$ J
$a_4 = 1.9\times10^{-18}$ J	
$T_0 = 2.6\times10^{2}$ K	$T_m = 3.1\times10^{2}$ K
$W = 1.9\times10^{-22}$ J	$w = 4.8\times10^{-24}$ J
$H = 1.0\times10^{-1}$ J m^{-2}	$h = 3.1\times10^{-20}$ J
$\Lambda_h = 2.5\times10^{-10}$ m	
$\varepsilon_0 = 8.9\times10^{-12}$ F m^{-1}	$\varepsilon_w = 80$
$q = 1.6\times10^{-19}$ C	$k_B T = 4.1\times10^{-21}$ K
$a_2'/h = 7.7\times10^{-2}$	$a_3/h = -30$
$a_4/h = 60$	$w/h = 1.6\times10^{-4}$[a]
$\lambda_h = 0.07$	

[a]The number for w/h given in Ref. 13 contains an error.

If we expand F_c as a power series in ψ, we see that interaction act as an external field on the order parameter ψ.[13] However, we treat the total free energy (13) in the following calculation.

For the purpose of calculating the phase diagrams of the lamellar system, we first minimize the total free energy density (13) with respect to ψ. Based on the equality of the chemical potentials and the osmotic pressures, the common tangent construction is employed to calculate the equilibrium between two phases with different ϕ' and ϕ''. In the coexisting two phases, the minimized order parameter ψ can take on different values from which the membrane thickness δ is calculated using (2). The incompressibility condition (1) further determines the thickness of the aqueous region d for given ϕ. These calculations have been done numerically. In order to determine the phase equilibria between a lamellar structure and excess water, the free energy of the latter solution is necessary as a function of the lipid composition. However, since this phase is extremely dilute in lipid, its free energy can be identified with that of pure water.[13] Hence the approximate coexistence for the equilibrium with excess water is determined by the condition of vanishing chemical potential, i.e., $\mu=0$. More rigorous treatment of the phase equilibrium should take into account the so-called Donnan equilibrium[20] which will be discussed in Sec. IV.

The numerical values of the model parameters used in the present calculation are summarized in Table I. For the quantities which are also used in Ref. 13, we choose the same numerical values in order to see the effect of the added term (10) clearly. In principle, the internal structural transition of the lipid bilayer may be affected by the electrostatic interaction through the modification of a_2, a_3, or a_4 as well as T_0 in (3). Furthermore, the added electrostatic interaction can give rise to the liner term in ψ in the Landau expansion of the stretching free energy. In such a case, the electrostatic interaction acts as an external field on the order parameter. The free energy is then shifted in a way which favors different membrane thickness. However, we do not consider these possibilities in this article since we want to focus on the effect of the electrostatic interaction only through the modification of the intermembrane interaction.

Strictly speaking, the temperature dependence of the present model appears both in F_L [Eq. (3)] and $V_e(d)$ [Eq. (10)] as well as in Λ_D [Eq. (8)]. For the simplicity, however, we fix the value of $k_B T$ in $V_e(d)$ and Λ_D to that given in Table I, and the temperature dependence is taken into account only through a_2 (or a_2/h). With these assumptions, we will see later in Sec. III that the melting transition (or, more precisely, the three phase coexistence temperature between the L_α, L_β, and excess water) occurs at $a_2/h = a_2'(T_m - T_0)/h \approx 3.33$. According to the experiments on the DMPC/water binary system,[3,13] the main transition temperature is $T_m = 310$ K and $T_m - T_0 = 50$ K (see Table I). Hence, from (4), each unit of the dimensionless temperature variable a_2/h corresponds to 15 K.[13]

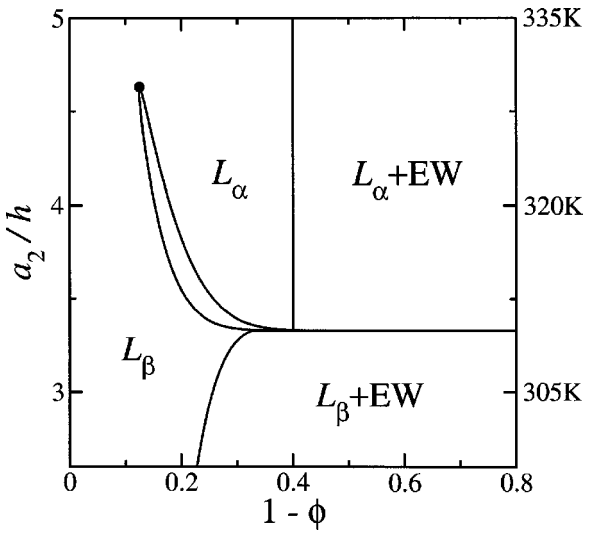

FIG. 2. Phase diagram of a mixture of neutral lipid and water. $1-\phi$ represents the water volume fraction, and a_2/h corresponds to the temperature. Equilibrium with excess water is denoted by "EW." The critical point is indicated by a filled circle. This phase diagram is the same with Fig. 5 in Ref. 13.

With the above choice of parameters, the reduced (dimensionless) Debye–Hückel screening length [see (12)] as a function of the number density of the electrolyte n_0 in units of [mol m^{-3}] is given by

$$\lambda_D = 2.78\times n_0^{-1/2}. \tag{16}$$

Using this relation, the ratio of parameters e/h is calculated to be

$$e/h = 0.016\times n_0^{1/2}. \tag{17}$$

III. RESULTS AND COMPARISON TO EXPERIMENTS

In this section, we show the calculated phase diagrams based on the free energy (13). The phase diagrams are represented in the $(1-\phi, a_2/h)$-plane, where $1-\phi$ is the water volume fraction and a_2/h corresponds to the reduced temperature. We focus on the variation of the phase behavior as the electrolyte concentration is varied.

As a reference, we reproduce in Fig. 2 the same phase diagram with that calculated by Goldstein and Leibler in Ref. 13 for the neutral lipid plus water binary system. This case corresponds to the limit of the charged lipids when $V_e(d) \to 0$ for all d. A line of first-order transition between the L_α and L_β phases terminates at a triple point where these two lamellar phases coexist with excess water. The narrowness of

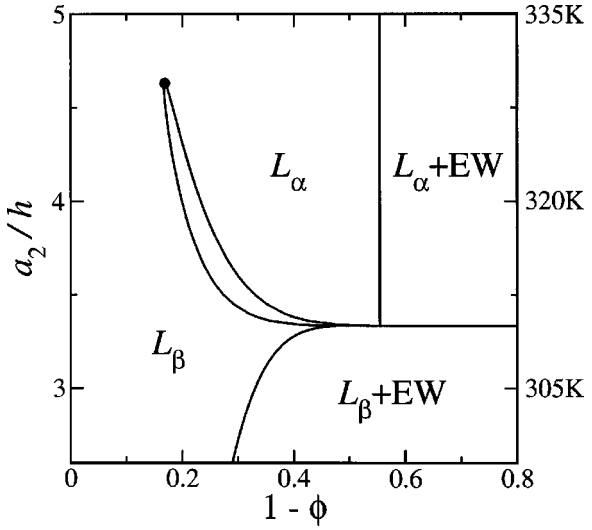

FIG. 3. Phase diagram of a mixture of charged lipid and water. The concentration of the added electrolyte is $n_0=5\times10^2$ mol m^{-3} (0.5 M). $1-\phi$ represents the water volume fraction, and a_2/h corresponds to the temperature. The notations of different phases are the same with Fig. 2. The critical point is indicated by a filled circle.

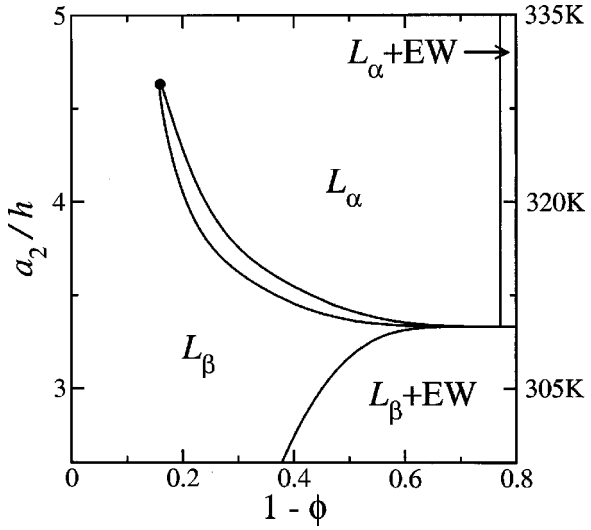

FIG. 4. Phase diagram of a mixture of charged lipid and water. The concentration of the added electrolyte is $n_0=1\times10^2$ mol m^{-3} (0.1 M). $1-\phi$ represents the water volume fraction, and a_2/h corresponds to the temperature. The notations of different phases are the same with Fig. 2. The critical point is indicated by a filled circle.

the tie lines persists to temperatures quite far from the critical point. Due to the skewing of this tilted two-phase region, a temperature scan at fixed composition crosses the two binodal lines. At higher temperature, the first-order line ends at the critical point (marked with a filled circle) beyond which the bilayer thickness changes continuously analogous to liquid/vapor type transition. Notice that the equilibrium swelling composition for the L_α phase is $1-\phi=0.4$, whereas it varies with temperature for the L_β phase.

Next we consider multilamellar dispersions consisting of charged lipid molecules and water. Figures 3 and 4 are the calculated phase diagrams for the electrolyte concentration $n_0=5\times10^2$ mol m^{-3} (0.5 M) and 1×10^2 mol m^{-3} (0.1 M), respectively. It is remarkable that the equilibrium swelling composition shifts to larger $1-\phi$ (or smaller ϕ) by decreasing the electrolyte concentration. For $n_0=1\times10^2$ mol m^{-3} (Fig. 4), the L_α phase can be swelled as large as $1-\phi\approx0.77$ water composition. As a result, the region of the single lamellar phases extends to the lower lipid composition regime. While the locus of the critical point does not change appreciably for different electrolyte concentrations, the compositions of the L_α and L_β phases at the triple point temperature shift to larger $1-\phi$. Hence, for small electrolyte concentration n_0, the two-phase region between the L_α and L_β phases is rather elongated, and the tie lines become narrower. As has been stated before, the temperature dependence of the present model is taken into account only through $a_2(T)$. Hence, compared to the neutral lipid case, the addition of the electrostatic interaction does not modify the temperature at the critical point or the triple point.

Our results reproduce several features of the experimentally studied phase diagram reported in Ref. 8 for charged lipid bilayer membranes. In Fig. 6 of Ref. 8, the temperature-composition phase diagram of DMPS/water binary system with added 0.025 M ammonium phosphate is determined by using differential scanning calorimetry. In the absence of water, pure DMPS undergoes a crystal to liquid crystal transition at 340 K. With increasing the water content the transition between the L_α and L_β phases occurs at progressively lower temperature. It finally reaches a limiting value of 310 K at water content of $1-\phi\approx0.45$. Even though the multilayer stacking may be disordered at higher water content, the DMPS/water binary system does not phase separate up to around 70 wt % water amount.[8,9] Further dilution leads to a transition from a single lamellar phase to a two-phase region where vesicles coexists with excess water.[9] We see a quite similar behavior of the main transition temperature in Fig. 4 except that the critical point is not observed in the experiment. As mentioned in the previous section, this is because of the shortcoming of the scalar order parameter (2) which does not distinguish any intramembrane symmetry differences. The difficulty in observing the coexistence between the L_α and L_β phases in the experiment may be due to the narrowness of the binodal region as shown in Fig. 4.

In Fig. 5, we have plotted various lengths, namely, the lamellar repeat distance $d+\delta$, the thickness of the water region d, the thickness of the lipid bilayer δ, and the Debye–Hückel screening length Λ_D [see (8)] as a function of the electrolyte concentration n_0 when the L_α phase coexists with the excess water. In other words, we follow the shift of the coexistence line between the L_α phase and the excess water as the electrolyte concentration is varied. The thickness of the lipid bilayer δ is calculated from the minimized order parameter ψ [see (2)], and the thickness of the water region d should satisfy the incompressibility condition (1). For the L_α phase, we remind that the swelling composition does not depend on temperature a_2/h (see Figs. 3 and 4). Figure 6 is the corresponding plot for the L_β phase coexisting with excess water at fixed $a_2/h=2.8$. We remark again that the coexistence line between the L_β phase and the excess water depends on the temperature a_2/h. For both the L_α and L_β phases, the thickness of the charged lipid bilayer δ (dotted

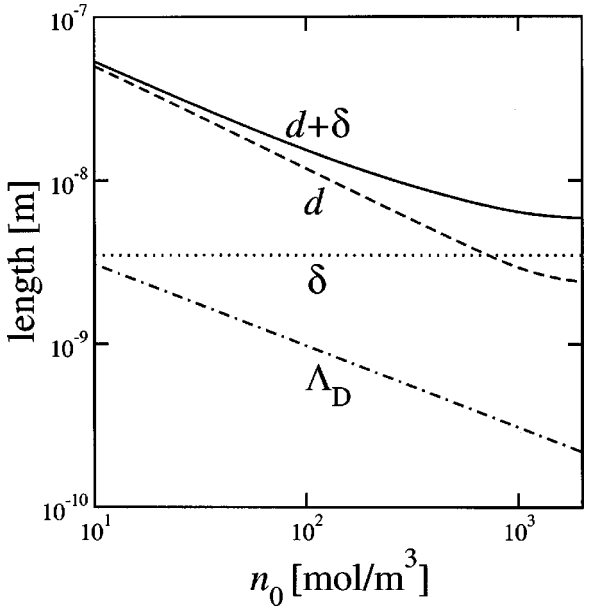

FIG. 5. Various lengths as a function of the electrolyte concentration n_0 when the L_α phase coexists with excess water. The solid line is the lamellar repeat distance $d+\delta$, the dashed line is the thickness of the water region d, the dotted line is the thickness of the lipid bilayer δ, and the dot-dashed line is the Debye–Hückel screening length Λ_D.

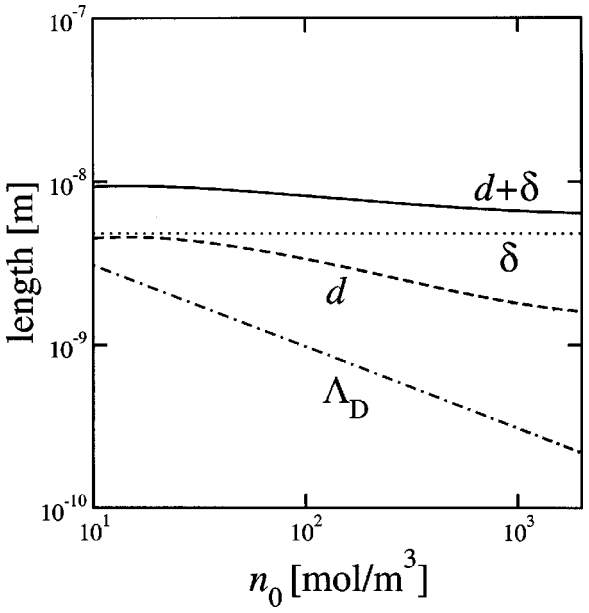

FIG. 6. Various lengths as a function of the electrolyte concentration n_0 when the L_β phase coexists with excess water at $a_2/h=2.8$. The notations of different lines are the same with Fig. 5.

line) does not change even if n_0 is varied. On the other hand, the thickness of the aqueous region d (dashed line) decreases as n_0 is increased. This tendency can be easily understood by noticing that the electrostatic repulsion between the membranes becomes more screened for larger n_0, and the intermembrane distance takes smaller value. For the L_α phase in Fig. 5, the lamellar repeat distance $d+\delta$ decreases as $n_0^{-0.52}$ and starts to level off around $n_0 \approx 0.5 \times 10^3\,\mathrm{mol\,m^{-3}}$ (0.5 M). The level off of the lamellar repeat distance can be explained as follows: Although the screened electrostatic repulsion becomes very weak for such a high electrolyte concentration, the hydration repulsion starts to dominate for small intermembrane distances.

The effect of monovalent cations on the phase behavior of DMPS/water binary system was investigated in Ref. 10. It is reported that the main transition temperature as well as the transition enthalpy remained almost unchanged as long as the added NaCl concentration does not exceed 1 M. Analysis of the x-ray diffraction data confirmed that, even in the presence of added NaCl, no significant change in the hexagonal hydrocarbon chain packing occurs in the L_β phase. The major effect of added salt is the electrolyte-concentration-dependent reduction in the lamellar periodicity as the water is excluded from the intermembrane space. For 50 wt% aqueous dispersion of DMPS, the lamellar repeat distance of the L_β phase at 293 K decreased linearly with increasing NaCl concentration up to 0.5 M and then leveled off (see Fig. 5 in Ref. 10). Compared to the electrolyte-free case, the lamellar periodicity reduced from 107 to 62 Å upon the addition of 0.5 M NaCl. The corresponding reduction in the lamellar periodicity of the L_α phase was from 75 to 52 Å. We consider that the above experiment has been done under the situation where the lamellar phase coexists with excess water. Otherwise the lamellar repeat distance is solely determined by the relative composition between lipid and water since the lipid bilayer thickness remains almost constant even if the electrolyte is added [see (1)]. Interestingly, the electrolyte concentration dependence of the repeat distance $d+\delta$ in Figs. 5 and 6 shows a similar behavior with the above mentioned experiment.

In Figs. 5 and 6, we see that the thickness of the aqueous region d is larger than the Debye–Hückel screening length Λ_D. Moreover both of these lengths are much larger than the Gouy–Chapman length $b \approx 1.5 \times 10^{-10}$ m as discussed in the previous section. These have been a necessary condition to use the asymptotic form of the electrostatic interaction given by (10). Hence our calculated results are consistent with the requirement for the intermediate region. However, for n_0 smaller than 1 mol m^{-3} in the L_β phase (not shown in the graph), d is calculated to be smaller than Λ_D, and it is no more appropriate to use (10). For such a small electrolyte concentration case, we are already either in the Gouy–Chapman region or the ideal-gas region, which will be discussed in the next section.

Fixing the electrolyte concentration to $n_0 = 1 \times 10^2\,\mathrm{mol\,m^{-3}}$ (0.1 M), we have plotted in Fig. 7 the lamellar bilayer repeat distance $d+\delta$ as a function of the water content $1-\phi$ at two different temperatures, i.e., $a_2/h=2.8$ and 4.4. This result is even in quantitative agreement with Fig. 7 in Ref. 8. For both the L_α and L_β phases, the bilayer repeat distance expands continuously as the water amount is increased. Compared to the L_α phase, the L_β phase takes larger repeat distance $d+\delta$ as well as the bilayer thickness δ. Since we have the constraint of the incompressibility condition (1), larger δ in the L_β phase means a denser lateral packing of the head groups in spite of the expected electrostatic repulsion between the charged groups. Such a reduction of the area per

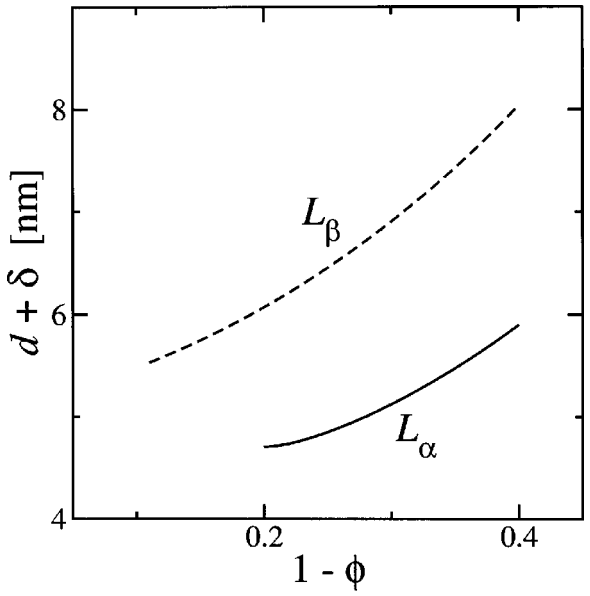

FIG. 7. The bilayer repeat distance $d+\delta$ as a function of the water content $1-\phi$ when $n_0=1\times10^2$ mol m^{-3} (0.1 M). The solid line is the repeat distance of L_α phase at $a_2/h=4.4$, and the dashed line is that of L_β phase at $a_2/h=2.8$.

molecule in the mixture of egg lecitin and charged lipid was observed in Ref. 5.

IV. DISCUSSION

In this article, we have investigated the phase behavior of the aqueous solution of charged lipid bilayer membranes forming a lamellar structure. We have focused on the effect of the added electrolyte. The Goldstein–Leibler model[13] proposed for the neutral lipids has been extended by taking into account the screened electrostatic interaction. Among various asymptotic regions of the Poisson–Boltzmann theory, we considered the so-called intermediate region. We paid attention to the variation of the phase behavior as the added electrolyte concentration is changed. With decreasing the electrolyte concentration (weak screening), the electrostatic repulsion between the neighboring membranes becomes stronger. Accordingly, the maximum equilibrium swelling composition shifts to larger water content, and the lamellar repeat distance increases although the membrane thickness remains almost constant. Our results recover not only the experimentally observed phase diagram for the charged lipid, but also the dependence of the lamellar repeat distance on the electrolyte concentration as well as on the lipid composition.

In our calculation, we have used the asymptotic form of the electrostatic interaction in the intermediate region as given in (10). It is valid when $b\ll\Lambda_D\ll d$, where Λ_D is the Debye–Hückel screening length (8), b is the Gouy–Chapman length (9), and d is the intermembrane distance. This condition is satisfied when the separation between the membrane is large compared to Λ_D although the Poisson–Boltzmann equation itself cannot be linearized since the surface potential is large. Notice that the asymptotic form of free energy does not depend on the surface charge density in this limit.

There are three other asymptotic regimes of the Poisson–Boltzmann theory represented in the $(\Lambda_D/d, b/d)$-parameter space:[16] (i) Debye–Hückel region [$\Lambda_D\ll b$ and $\Lambda_D/d\ll1$, or $(\Lambda_D/d)^2\ll b/d$ and $\Lambda_D/d\gg1$], (ii) ideal-gas region [$b/d\gg1$ and $(\Lambda_D/d)^2\gg b/d$], and (iii) Gouy–Chapman region [$b/d\ll1$ and $\Lambda_D/d\gg1$]. In the Debye–Hückel region, the potential value on the membrane surface is small, and the Poisson–Boltzmann equation can be linearized. The resulting asymptotic form of the energy per unit area is then

$$V_e(d)=\frac{\sigma^2\Lambda_D}{\varepsilon_0\varepsilon_w}\left[\coth\left(\frac{d}{2\Lambda_D}\right)-1\right], \tag{18}$$

where σ is the surface charge density as before. By replacing (10) with (18) and looking at the total interaction energy as a function of d (with an appropriate choice of σ), we have confirmed that the phase behavior is not modified at least qualitatively. This is a natural consequence since both (10) and (18) are exponentially decaying functions.

For the ideal-gas and the Gouy–Chapman regions, on the other hand, the repulsive interaction energy decays algebraically rather than exponentially. In contrast to the intermediate region, it was impossible to construct a globally consistent phase diagram due to the long-ranged nature of the interaction as long as we use reasonable numerical values of model parameters. When the repulsive interaction is too strong, the typical intermembrane distance becomes much larger than the membrane thickness. In such a highly swollen case, the internal and the external degrees of freedom of the membranes do not couple each other. It is then reasonable to assume that membranes are infinitesimally thin homogeneous layers characterized by coarse-grained elastic properties. We encounter a similar situation when one takes into account the long-range Helfrich steric interaction which decays also algebraically.[21]

When we calculated the phase equilibria between one of the lamellar phases and the excess water, only the condition of vanishing chemical potential ($\mu=0$) was used. Although this is justified for neutral lipids, further complication could arise for charged membranes in the presence of the electrolyte. For example, due to the constraint of electroneutrality in the membrane system, there is a tendency for the added electrolyte to go into the less crowded excess water region. This phenomenon is known as the Donnan effect[20] which induces a difference in the average electrolyte concentration between the membrane system and the excess water.[22] As a result, an excess osmotic pressure difference should arise between the two phases,[23] and the location of the phase boundary would possibly be modified. In order to consider such a problem, however, one should treat the electrolyte concentration as an additional degree of freedom, and the chemical potential of the electrolyte should be taken into account. However, this is out of the scope of the present model. Similar argument holds also for the phase equilibrium between the L_α and $L_{\beta'}$ phases since the intermembrane distance is different for these phases. We note that the Donnan effect becomes more important for highly charged membranes.

In the present study we have neglected not only the difference between the L_β and $L_{\beta'}$ phases, but also the presence

of the so called rippled ($P_{\beta'}$) phase where the membrane structure is modulated. The rippled phase, when it exists, lies typically between the L_α and $L_{\beta'}$ phases. Recent experiment shows that the $P_{\beta'}$ phase exhibits anomalous dielectric properties due to the strong dipole–dipole correlation.[24] In order to consider such a modulated phase, one needs to use a space-dependent order parameter. Moreover, it is more appropriate to use a vector order parameter rather than the scalar order parameter.[25] The study to obtain the full phase behavior of the aqueous solution of lipid bilayer membranes is under progress.

ACKNOWLEDGMENTS

We thank D. Andelman and K. Fukada for useful discussions. This work is supported by the Ministry of Education, Culture, Sports, Science and Technology, Japan (Grant-in-Aid for Scientific Research No. 13740257).

[1] D. Marsh, *Handbook of Lipid Bilayers* (CRC, Boca Raton, FL, 1990).
[2] *Structure and dynamics of membranes: Generic and specific interactions*, Vol. 1B of *Handbook of Biological Physics*, edited by R. Lipowsky and E. Sackmann (Elsevier, Amsterdam, 1995).
[3] M. J. Janiak, D. M. Small, and G. G. Shipley, J. Biol. Chem. **254**, 6068 (1979).
[4] N. Markova, E. Sparr, L. Wadsö, and H. Wennerström, J. Phys. Chem. B **104**, 8053 (2000).
[5] A. C. Cowley, N. L. Fuller, R. P. Rand, and V. A. Parsegian, Biochemistry **17**, 3163 (1978).
[6] M. E. Loosley-Millman, R. P. Rand, and V. A. Parsegian, Biophys. J. **40**, 221 (1982).
[7] D. Atkinson, H. Hauser, G. G. Shipley, and J. M. Stubbs, Biochim. Biophys. Acta **339**, 10 (1974).
[8] H. Hauser, F. Paltauf, and G. G. Shipley, Biochemistry **21**, 1061 (1982).
[9] H. Hauser, N. Gains, and D. D. Lasic, in *Physics of Amphiphiles: Micelles, Vesicles and Microemulsions*, edited by V. Degiorgio (North-Holland, Amsterdam, 1985).
[10] H. Hauser and G. G. Shipley, Biochemistry **22**, 2171 (1983).
[11] G. Cevc, A. Watts, and D. Marsh, Biochemistry **20**, 4955 (1981).
[12] R. E. Goldstein and S. Leibler, Phys. Rev. Lett. **61**, 2213 (1988).
[13] R. E. Goldstein and S. Leibler, Phys. Rev. A **40**, 1025 (1989).
[14] R. P. Rand, Annu. Rev. Biophys. Bioeng. **10**, 277 (1981).
[15] J. Israelachivili, *Intermolecular & Surface Forces* (Academic, New York, 1992).
[16] D. Andelman, in Ref. 2, pp. 603–642.
[17] J. M. Collins, B. A. Cunningham, D. H. Wolfe, W. Tamura-Lis, L. J. Lis, O. Kucuk, and M. P. Westerman, J. Colloid Interface Sci. **153**, 592 (1992).
[18] P. Pincus, J.-F. Joanny, and D. Andelman, Europhys. Lett. **11**, 763 (1990).
[19] J. L. Harden, C. Marques, J.-F. Joanny, and D. Andelman, Langmuir **8**, 1170 (1992).
[20] F. G. Donnan, Chem. Rev. (Washington, D.C.) **1**, 73 (1924).
[21] W. Helfrich, Z. Naturforsch. A **33A**, 305 (1978).
[22] M. Deserno and H.-H. von Grünberg, Phys. Rev. E **66**, 011401 (2002).
[23] M. Dubois, T. Zemb, L. Belloni, A. Delville, P. Levitz, and R. Setton, J. Chem. Phys. **96**, 2278 (1992).
[24] A. Raudino, F. Castelli, G. Briganti, and C. Cametti, J. Chem. Phys. **115**, 8238 (2001).
[25] C.-M. Chen, T. C. Lubensky, and F. C. MacKintosh, Phys. Rev. E **51**, 504 (1995).